sciendo Slovak Journal of Civil Engineering
Vol. 33, 2025, No. 2, 1 – 10
DOI: 10.2478sjce-2025-0007

STUDY OF THE EFFECT OF WIND FLOW AROUND THE RUIN OF A FORTIFIED TOWER VARIOUSLY COVERED BY A FLAT ROOF: ANALYSIS OF THE EXTREME VALUES OF EXTERIOR PRESSURE AND SURFACE FRICTION COEFFICIENTS

Martin POLIAK[1*], Michal FRANEK[2], Jana GREGOROVÁ[1]

Abstract

An analysis of the effect of the covering of a ruin by a flat roof of various sizes and positions is presented. The ruin has almost cube-like proportions, with an open roof plane and an open destroyed corner. The coverage of the ruin by a roof is viewed as protection against wind and its associated destructive mechanisms. The effect of the wind flow is illustrated by the minimum and maximum values of the external pressure and the skin friction coefficients. Taking the changes of these values into account, the degree of protection of the ruin by the flat roof alternatives is estimated, and the optimal alternative for the coverage is discussed. Simulations of the wind study were conducted using the Fluent by Ansys, computational fluid dynamics software, 3D Time Steady Reynolds-Averaged Navier-Stokes equations, and the Shear Stress Transport k-ω turbulence model.

Address

[1] Dept. of Architecture, Faculty of Civil Engineering, Slovak University of Technology in Bratislava, Slovak Republic

[2] Dept. of Building Construction, Faculty of Civil Engineering, Slovak University of Technology in Bratislava, Slovak Republic

* ***Corresponding author:*** martin.poliak@stuba.sk

Key words

- Ruin protection,
- Wind flow simulation,
- Computational fluid dynamics,
- Ruin coverage.

1 INTRODUCTION

A building is stressed by the joint action of a spectrum of destructive mechanisms. Without any maintenance, it is eventually degraded to a state of ruin. Wind is one of the primary sources of natural destructive mechanisms with both gradual and sudden durations of its action (Makýš 2018), (How 2007). The wind is also one of the main distributors of other sources of destructive mechanisms (How 2007), (Sesana, Gagnon, Ciantelli, Cassar, Hughes 2021), (Sabbioni, Brimblecombe, Cassar 2010). As such, the action of wind is of a mechanical and chemical character, as the wind collaborates in changing the surface integrity of an object by grinding its surface and removing its loosened elements. The wind also creates dynamic loads on the structure of the object and alters chemical reactions from water and gas inside of an object by changing their pressure and by transporting contained impurities. As objects in an advanced decayed state, ruins are highly sensitive to the effects of destructive mechanisms and their further development (Sesana, Gagnon, Ciantelli, Cassar, Hughes 2021). This sensitivity is caused by the natural complexity of their geometry and by the quality of their building material (Shao, Li, Wang, Wang, Li 2013).

The degree to which ruins are exposed to wind-induced destructive action is closely related to the position of the coverage, relative to the ruin. The resulting proportion, shape and geometric relationship between the two bodies and their changes are of interest (Bielek, Franek, Bielek 2020), (Singh, Roy 2019), (Fouad, Mahmoud, Nasr 2018), (Mou, He, Zhao, Chau 2017). Two parameters are followed in more detail in this paper: the distance between the coverage and the ruin in a vertical direction and the size of the covering roof in either the size of its overlap or in its embedment behind the face of the ruin.

The present paper adds to considerations that have examined the effectiveness of covering structures over ruins as protection from further deterioration (Cabello-Briones, Mayorga-Pinilla, Vázquez-Moliní 2020), (Aslan, Court, Teutonico, Thompson 2018), (Soria, Guerrero, García 2017), (Yaka Çetin, Ipekoĝlu 2013). Philosophically, it relies on studies that are similar in topic (Fortunato, Frega, Lauria, Zappani 2024), (Kim 2023), (Pineda, Iranzo 2017), (Hussein, El-Shishiny 2009), that have considered monument material as a backbone of culturally and ecologically sustainable development and a means of protection of the genius loci (Vecco 2020), which is reflected in various spatial scales and origins (Antrop 2006), (D'Acci 2019), (Ruhigová, Ruhig, Gregorová 2024), (Bránický, Gregorová 2022).

More specifically, the paper analyses the effectiveness of flat structures placed directly on a ruin with various values of distance and size. The effect it brings on a wind flow and its action on the surface of a ruin is illustrated with the aid of a wind study that uses a computational fluid dynamics model and a method validated experimentally and statistically in a previous paper (Poliak, Franek, Gregorová 2023). To do so, this study analyses the minimum and maximum values calculated of the external pressure and the skin friction coefficients and changes they undergo when inflicted by variations of a covering flat roof.

2 MATERIALS AND METHODS

An idealised model of the ruin of the southeastern tower of the Trnava (Slovakia) fortifications is utilised in the study; it had previously been identified as a location of high cultural value, which is currently undergoing the actualisation of its monumental presentation (Gregorová, Vojteková 2022). Various solutions of covering it by a roof have been analysed in previous works from an architectural-monumental point of view (Poliak 2022), (Poliak, Gregorová, 2022). The ruin of interest, its location, and the creation and idealisation of its model used in a wind study has been followed in detail in previous works (Poliak, Franek, Gregorová 2023) (Fig. 2).

Fig. 1 Picture of the ruin of interest of Trnava's fortified southeastern tower in its actual state in 2021. The point of view is northwest of the interior of the fortification.

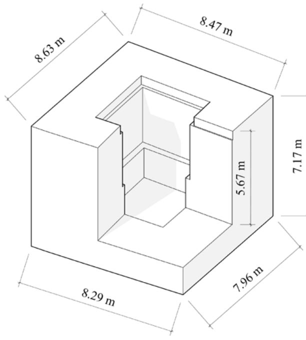

Fig.2 The model of the ruin of interest of Trnava's fortified tower in its idealised state.

Two parameters of the ruin-coverage relationship, i.e., the distance between the coverage and the ruin in the vertical direction and the size of the covering roof in either the size of its overlap, or its embedment behind the face of the ruin, are followed in detail. The characteristic multiple of the two parameters was chosen as 0.5 m, as it represents a quarter of the masonry's thickness. The values of the size of the roof overlap are considered from -1.5 m to +2.0 m (see branches A-H in Fig. 3). The distance of the two bodies is considered from 0.0 m to +2.0 m (see branches 1-5 in Fig. 3).

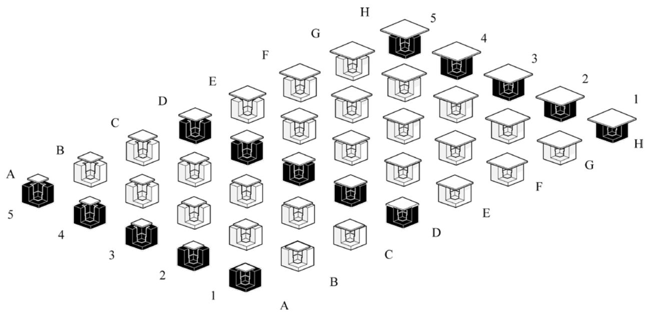

Fig.3 A matrix of the flat roofs considered with various sizes and with various distances from the ruin model; the branches simulated in the wind study are marked in black.

Wind flow simulations were performed around three of the matrix branches: branch A with a maximum embedment of the roof, branch D without the overhang of the roof, and branch H with a maximum overhang (Fig. 3). The wind flow simulations were performed using ANSYS Fluent software. The dimensions of the computational domain were 2.6 × 1.6 × 4.8 m and were based on the maximum dimension of the idealised model (Franke, 2007) on a scale that was previously used in the calibration of the computational procedure by comparing the results of the exterior pressure coefficient cpe with the experimental measurements. The computational mesh was polyhedral with the growth rate and sizing limited to 1.1, with the assignment of the smooth transition inflation conditions for the first five layers above the terrain surface, and with the first layer thickness inflation for the first five layers with a thickness of the first layer of 1 mm and a sizing of 1 mm for the surface of the idealised ruin model, as well as the roofing. The numbers of mesh nodes ranged from 1.67 to 2.92 million and the number of elements from 6.04 to 10.85 million (different rotations of the model when simulating multiple wind flow directions and different roof alternatives produced different numbers of mesh nodes and elements). There was a logarithmic wind profile with an aerodynamic roughness length of 0.7 m on the full scale set for the input area, symmetry with the zero gradients for the top and side planes of the computational domain, a uniform roughness of a height of 0.5 mm and a 0.5 roughness constant for the ruin model, and a 0.7 roughness constant for the terrain surface of height of 1.79 mm. A Reynolds-averaged Navier-Stokes shear stress transport k–ω calculation model was chosen, and flow simulations were performed as pressure-based and time steady with no production limiter, a curvature correction, and a maximum residue value set at 10^{-5}; see (Poliak et al., 2023) for further detail. The values of the exterior pressure coefficient c_{pe} and the surface friction coefficient c_f were monitored, as given by the equations:

$$c_{pe} = \frac{p - p_s}{\frac{1}{2}\rho v_{ref}^2} \quad (1)$$

$$c_f = \frac{\tau_w}{\frac{1}{2}\rho v_{ref}^2} \quad (2)$$

based on the local static pressure p [Pa], the free stream mean static pressure p_s [Pa], the air density ρ [kg·m^{-3}], the reference wind flow velocity v_{ref} [m·s^{-1}], and the local shear stress τ_w [Pa] (Bielek, Franek, Bielek 2020), (*Skin friction coefficient*).

The minimum and maximum values of the coefficients were observed separately on the surfaces of the head of the masonry (HM), which is generally stressed by high negative pressure values; the windward side (WW), which is mostly stressed by positive pressure, and the leeward side (LW). The values calculated from the direction of the wind flow given were compared to those obtained by simulating the wind flow around the ruin model without a roof. To assess the overall impact of the roof alternative given, the results from the three directions of wind flow given were averaged:

$$c_{pe,min/MAX,diff,A} = \frac{1}{3}\sum_{i=1}^{3}(c_{pe,min/MAX,XY,A,i} - c_{pe,min/MAX,O,A,i}) \quad (3)$$

$$c_{f,min/MAX,diff,A} = \frac{1}{3}\sum_{i=1}^{3}(c_{f,min/MAX,XY,A,i} - c_{f,min/MAX,O,A,i}) \quad (4)$$

where c_{pe} stands for the exterior pressure coefficient [-]; c_f for the surface friction coefficient [-]; *m/M* stands for the minimum or maximum value of the coefficient; *diff* stands for the difference in values between the original model of the ruin without a roof and the model covered by a roof; *A* stands for the area of interest (HM, WW, or LW); XY stands for the roof alternative in Fig. 3; *O* stands for the original alternative without a roof; and i stands for the direction of the wind (Poliak, Franek, Gregorová 2023).

The impact of the uncalculated alternatives (Fig. 3) was estimated by interpolation.

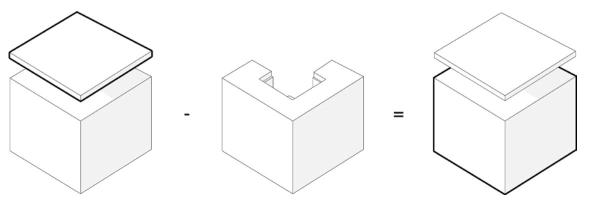

Fig.4 *An illustration of the methodology of the validation of the results, as given by equations (3) and (4)*

3 RESULTS

The results of the study are illustrated by histograms for the sake of the readability of the development of the effects of the coverage of the ruin model by each XY alternative of the flat roof. The size alternatives are arranged from the maximum embedment of the roof behind the face of the model to the maximum overhang of the roof from the branch A to the branch H. The distance alternatives of the roof are grouped by the size branches from 1 (the roof in contact with the ruin model) to 5 (the roof with a maximum distance of the roof) (see also Fig. 3). First, the results for the surface of the head of the masonry (HM) are shown and described; then the WW and LW surfaces are shown and described.

3.1 The head of the masonry (HM)

Fig. 5 shows a histogram of the mean changes in the minimum values of the exterior pressure coefficient on the HM surface of the ruin model $c_{pe,min,diff,HM}$. The change from the positive to negative values between alternatives 2-4 points to the negative effect of too much distance between the roof and the model. The increase in the mean changes between the branches A-H points to the linear relativity between the size of the positive change in the negative pressure on the head surface and the size of the roof, although the relativity is not constant between the A-D branches and the D-H branches. The almost constant pattern of development between the D-H branches shows that the size of the covering roof has little effect on the same distance of the roof from the model. The greatest impact is caused by the D1-H1 alternatives, which completely cover the HM. The effect of the D2-H2 alternatives is also significant (from +0.529 to +0.588 in total, or from -19.3% to -21.3%).

Fig. 6 shows a histogram of the mean changes in the maximum values of the exterior pressure coefficient on the HM surface of the ruin model $c_{pe,MAX,diff,HM}$. No constant pattern of development in the values was recorded between the distance branches 15 nor between the size branches A-H. Only the H branch points to the dependency of the decrease in the values of the changes on the distance of the roof and the model. The greatest impact is caused by the D1-H1 alternatives, which completely cover the HM. The effect of H2 alternative is also significant (+0.218 in total, or -74.5%).

Fig. 7 shows a histogram of the mean changes in the minimum values of the surface friction coefficient on the HM surface of the ruin model $c_{f,min,diff,HM}$. The almost constant pattern of development between the A-D branches points to little dependency between the change values and the size of the embedment of the roof. This pattern changes towards branch H. The greatest impact is caused by the D1-H1 alternatives, which completely cover the HM. The second greatest impact is caused by the H2 alternative (+1.54·10-3 in total, or -2663.2%). The changes by the other alternatives remain close to the zero value.

Fig. 8 shows a histogram of the mean changes in the maximum values of the surface friction coefficient on the HM surface of the ruin model $c_{f,MAX,diff,HM}$. The A-H pattern of development points to the dependency in the yield of the change in the values and the size of the roof – only the D2-H2 alternatives break the pattern. The greatest impact is caused by the D1-H1 alternatives, which completely cover the HM. The second greatest impact is caused by the D2 alternative (-9.16·10-3 in total, or -15.0%).

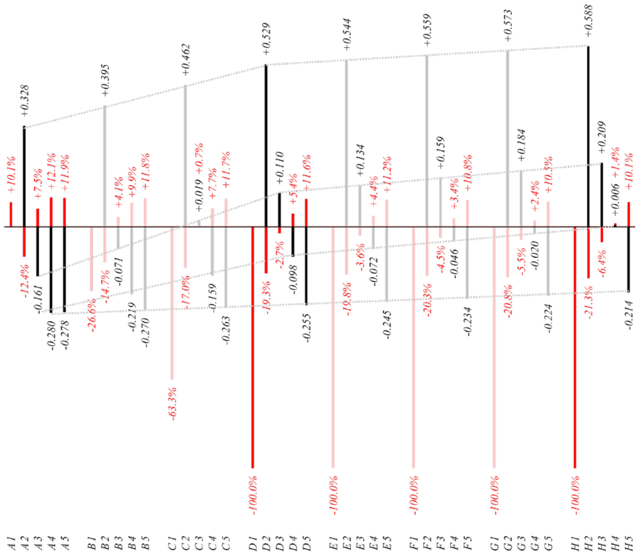

Fig.5 *A histogram of the mean changes in the minimum values of the exterior pressure coefficient on the HM surface of the ruin model* $c_{pe,min,diff,HM}$. *The development pattern between alternatives 2-5 points to the importance of the distance of the covering roof; the pattern between A-H (dotted line) suggests the size of the roof to be less of importance. The greatest impact is caused by the D1-H1 alternatives, which completely cover the HM. The effect of the D2-H2 alternatives is also significant.*

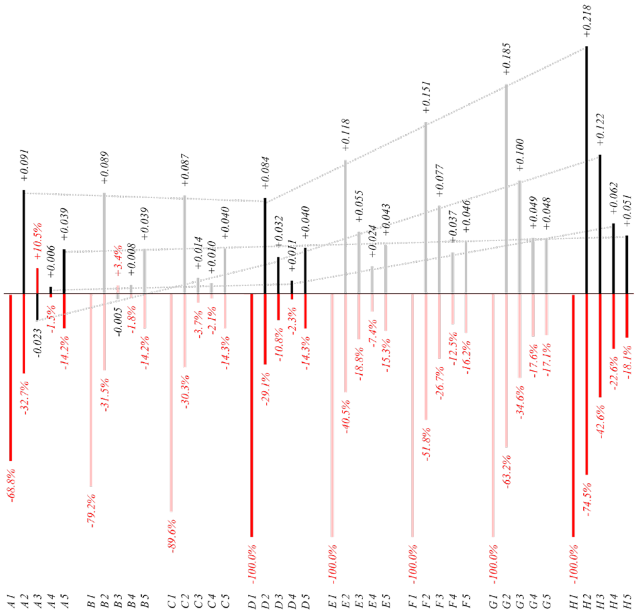

Fig.6 *A histogram of the mean changes in the maximum values of the exterior pressure coefficient on the HM surface of the ruin model* $c_{pe,MAX,diff,HM}$. *Aside from the H branch, no readable pattern of development is shown in the changes caused by the distance of the covering roof (branches 1-5), and no visible pattern is shown between the A-H branches (dotted line). The greatest impact is caused by the D1-H1 alternatives, which completely cover the HM. The effect of the H2 alternative is also significant.*

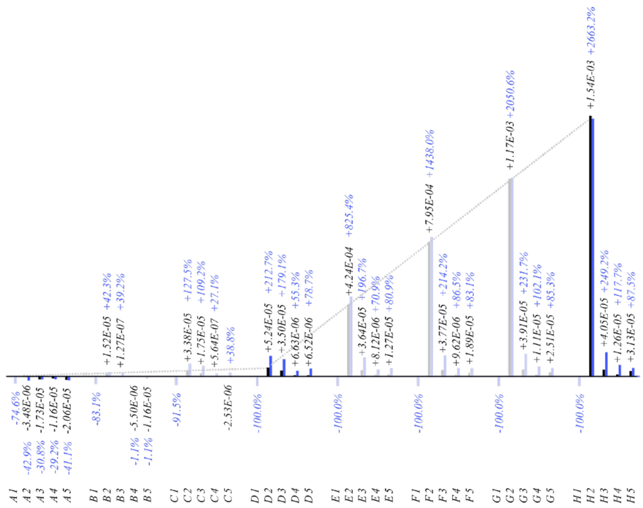

Fig.7 *A histogram of the mean changes in the minimum values of the surface friction coefficient on the HM surface of the ruin model* $c_{f,min,diff,HM}$. *Notice the almost constant pattern of development between the A-D branches (dotted line) and the almost zero total values of the mean changes (marked in black), which point to a little to no effect of the size of the embedment of the roof. The greatest impact is caused by the D1-H1 alternatives, which completely cover the HM. The second greatest impact is caused by the H2 alternative.*

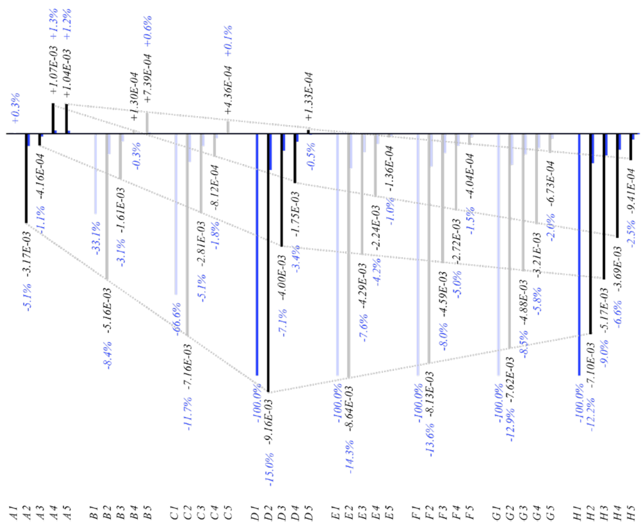

Fig.8 *A histogram of the mean changes in the maximum values of the surface friction coefficient on the HM surface of the ruin model* $c_{f,MAX,diff,HM}$. *Patterns 1-5 of the development point to the importance of the size of the roof. The A-H pattern (dotted line) is slowly inclined with the exception of the 2 alternatives. The greatest impact is caused by D1-H1 alternatives, which completely cover the HM. The second greatest impact is caused by the D2 alternative.*

3.2 The windward surfaces (WW)

Fig. 9 shows a histogram of the mean changes in the minimum values of the exterior pressure coefficient on the WW surface of the ruin model $c_{pe,min,diff,WW}$. No constant pattern of the development in the values was recorded by the study between the size branches A-H. However, the distance branches 1-5 point to one direction of development, which turns at the branch 2, which means that there is a positive impact from adding a small distance between the roof and the ruin, which slowly turns into a negative impact in relation to the size of the roof. The greatest impact is caused by the H2 alternative (+0.556 in total, or -22.6%).

Fig. 10 shows a histogram of the mean changes in the maximum values of the exterior pressure coefficient on the WW surface of the ruin model $c_{pe,MAX,diff,WW}$. The simulated size of branches A and D points to a little to no effect of the roof sizes that are smaller or similar in their area as the covered ruin. The pattern of development between the D-H branches point to the negative effect of adding an overhang to the roof, which gets smaller by increasing the distance of the roof (see branches 1-5). The greatest impact is caused by the H1 alternative, although it is not very significant in value (+0.099 in total, or +11.3%).

Fig. 11 shows a histogram of the mean changes in the minimum values of surface friction coefficient on the WW surface of the ruin model $c_{f,min,diff,WW}$. The pattern of development is intangible. Take notice of the near zero total values of the impacted changes. The data in the histogram are considered the noise of the calculation method used in the study, as the minimum value of the surface friction coefficient cf may equal zero, meaning that no part of the stream of the wind flow is parallel in a direction to the surface of the model of the ruin. The greatest impact is caused by the H2 alternative (+1.08·10-5 in total, or +64.4%).

Fig. 12 shows a histogram of the mean changes in the maximum values of the surface friction coefficient on the WW surface of the ruin model $c_{f,MAX,diff,WW}$. The pattern of development points to the positive impact of the coverage by a roof, which increases with the roof's size (see branches A-H) and decreases with the growing distance of the roof (branches 1-5). The greatest impact is caused by the H1 alternative ($-1.81\cdot10^{-2}$ in total, or -25.7%).

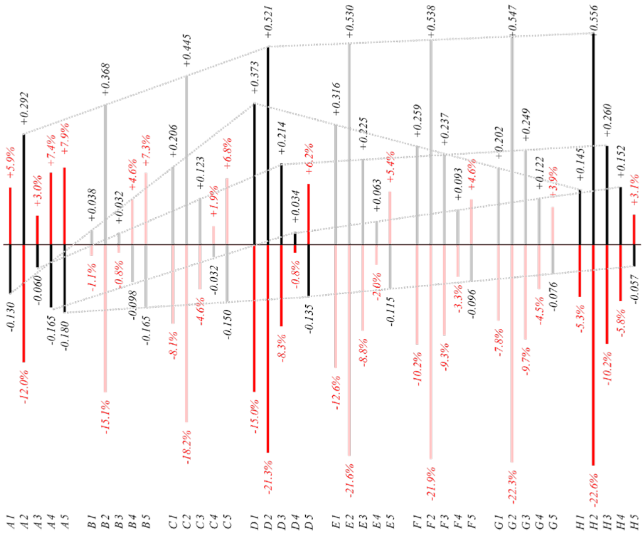

Fig.9 *A histogram of the mean changes in the minimum values of the exterior pressure coefficient on the WW surface of the ruin model cpe,min,diff,WW. Patterns 1-5 of the development point to the greatest impact of alternatives 2. No common pattern was recorded between the A-H branches (dotted line). The greatest impact is caused by the H2 alternative.*

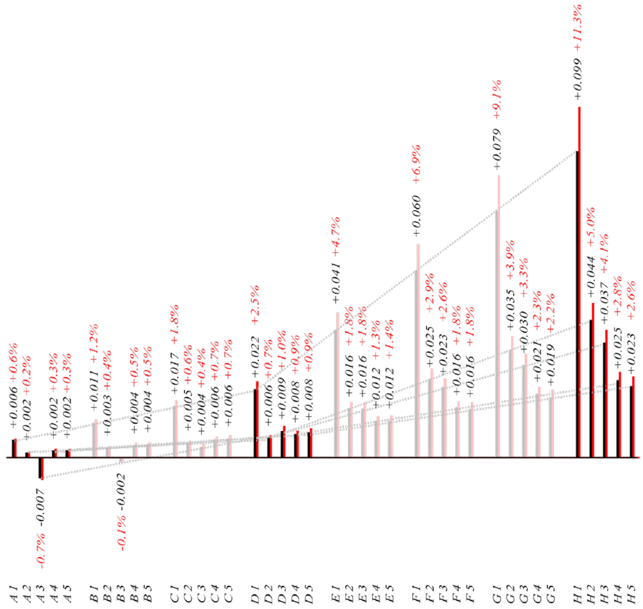

Fig.10 *AA histogram of the mean changes in the maximum values of the exterior pressure coefficient on the WW surface of the ruin model $c_{pe,MAX,diff,WW}$. No common pattern of development is shown between alternatives 1-5. The pattern between the A-H alternatives points to the importance of the size of the roof overhang (dotted line). The greatest impact is caused by the H1 alternative, although its total value is not very significant (marked in black).*

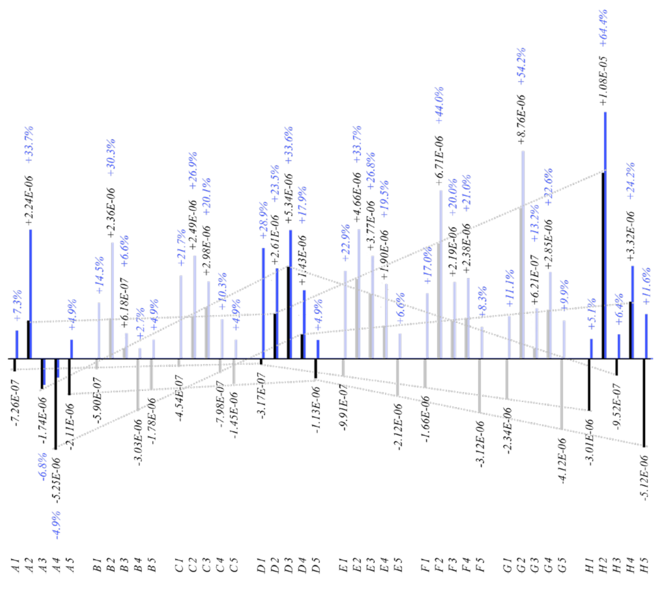

Fig.11 *A histogram of the mean changes in the minimum values of the surface friction coefficient on the WW surface of the ruin model $c_{f,min,diff,WW}$. No tangible patterns of development are shown between alternatives 1-5, nor branches A-H (dotted line). Notice the almost zero total values of the changes (marked in black). The greatest impact is caused by the H2 alternative.*

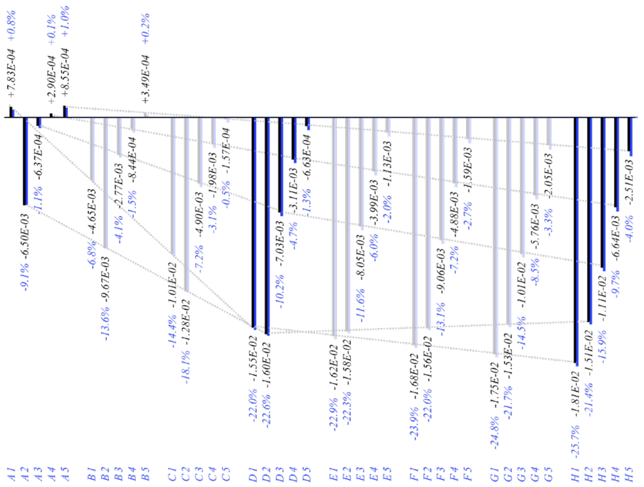

Fig.12 *A histogram of the mean changes in the maximum values of the surface friction coefficient on the WW surface of the ruin model* $c_{f,MAX,diff,WW}$. *The pattern of development between alternatives 1-5 point to the importance of the distance of the covering roof, and the pattern between the A-H branches point to the importance of the size of the roof (dotted line). The greatest impact is caused by the H1 alternative.*

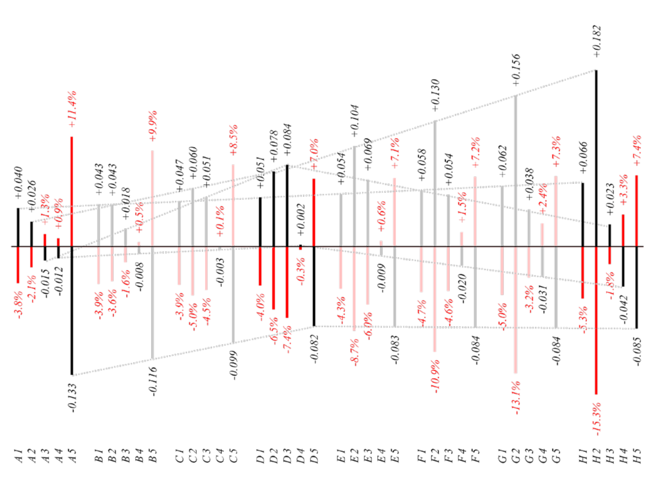

Fig.13 *A histogram of the mean changes in the minimum values of the exterior pressure coefficient on the LW surface of the ruin model* $c_{pe,min,diff,LW}$. *No common pattern of development is shown between alternatives 1-5, nor between branches A-H (dotted line). The greatest impact is caused by the H2 alternative.*

3.3 The leeward surfaces (LW)

Fig. 13 shows a histogram of the mean changes in the minimum values of the exterior pressure coefficient on the LW surface of the ruin model $c_{pe,min,diff,LW}$. No constant pattern of the development in the values was recorded by the methodology of this study. The greatest impact is caused by the H2 alternative (+0.182 in total, or -15.3%).

Fig. 14 shows a histogram of the mean changes in the maximum values of the exterior pressure coefficient on the LW surface of the ruin model $c_{pe,MAX,diff,LW}$. The branch 1 alternatives had little impact on the values. This changes when the roof increases in its size, as can be seen in most of the branches 2-5. The most positive values were achieved by alternatives H3 and D3. The greatest impact is caused by the H3 alternative (+0.293 in total, or -116.9%).

Fig. 15 shows a histogram of the mean changes in the minimum values of the surface friction coefficient on the LW surface of the ruin model $c_{f,min,diff,LW}$. Once again, no constant pattern of the development in the values was recorded, and the results are near zero in their real value. The greatest impact is caused by the D4 alternative (+8.17·10-7 in total, or +155.3%).

Fig. 16 shows a histogram of the mean changes in the maximum values of the surface friction coefficient on the LW surface of the ruin model $c_{f,MAX,diff,LW}$. No constant pattern of the development in the values was recorded between the branches of alternatives A-H. Branches 1-5 may point to the positive effect of the near positioning of the roof, although this pattern is not constant in each size of branches A-H. The most positive values were caused by the H1 and D1 alternatives. The greatest impact is caused by the H1 alternative (-9.52·10-3 in total, or -288.4%).

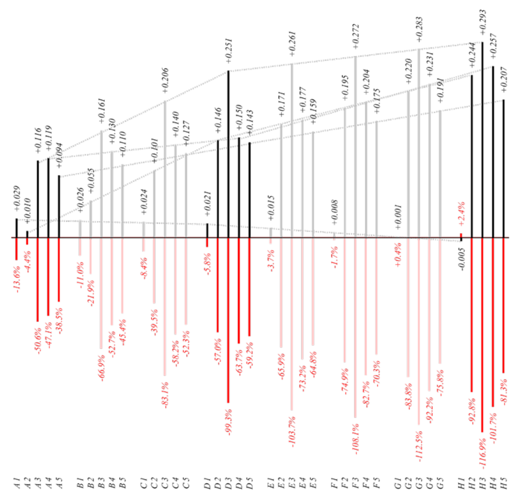

Fig.14 *A histogram of the mean changes in the maximum values of the exterior pressure coefficient on the LW surface of the ruin model* $c_{pe,MAX,diff,LW}$. *The pattern of development between alternatives 1-5 points to the optimal middle distance of the roof. The pattern between branches A-H points to the importance of the size of the roof (dotted line) with the exception of alternative 1, which yields a small total value of change (marked in black). The greatest impact is caused by the H3 alternative.*

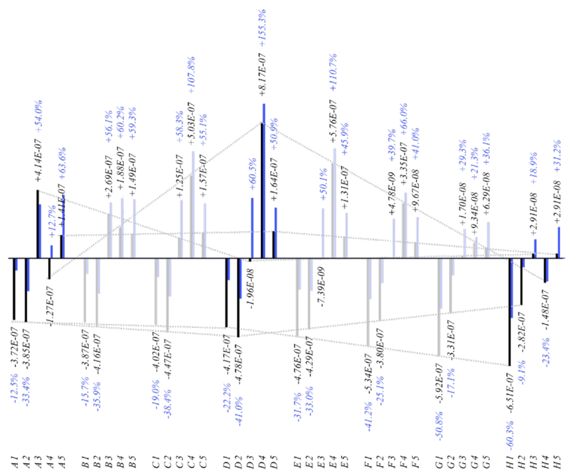

Fig.15 *A histogram of the mean changes in the minimum values of the surface friction coefficient on the LW surface of the ruin model $c_{f,min,diff,LW}$. No tangible patterns of development are shown between alternatives 1-5, nor between branches A-H (dotted line). Notice the almost zero total value of any changes (marked in black). The greatest impact is caused by the D4 alternative.*

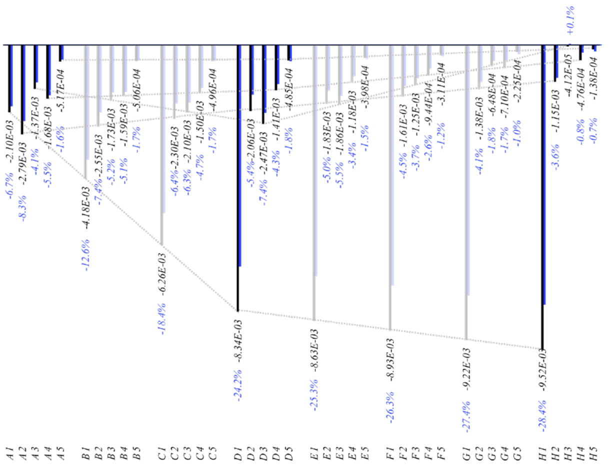

Fig.16 *A histogram of the mean changes in the maximum values of the surface friction coefficient on the LW surface of the ruin model $c_{f,MAX,diff,LW}$. The pattern of development between alternatives 1-5 points to the importance of the distance of the covering roof, although its character is not constant for each of the branches A-H. The pattern between the A-H branches does not point to readable results (dotted line). The greatest impact is caused by the H1 alternative.*

3.4 Summary of the results of the entire surface

On the HM, the greatest changes were caused by the D1-H1 alternatives, as they completely cover the surface. They were followed by the '2' alternatives, which usually caused the greater change with the larger size of the roof (with the exception of $c_{f,MAX}$ – see Fig. 8).

On the WW, the greatest changes are caused by the H alternatives. However, in cpe,min the pattern of development is not readable (see Fig. 9), and in $c_{pe,MAX}$, the values of change are insignificant. This is thought to be caused by a philosophic error of the study of the WW. $c_{pe,min}$ is usually located at the upper edge of the model, where the WW meets the HM. This edge is created by the substance of the ruin in its original state and by the material of the new roof in the covered state of the ruin; thus the changes in the values at the WW between the two states of the ruin may be quite random. The insignificant changes of $c_{pe,MAX}$ are due to the same maximum possible value (which is 1.0 in theory).

On the LW, the patterns for cpe,min and cf,min are once again incomprehensible for similar reasons as on the WW (see Figs. 13 and 15). Even though the patterns for $c_{pe,MAX}$ and $c_{f,MAX}$ are clearer, their pattern breaks the expectations set by HM and WW; for $c_{pe,MAX}$, the greatest changes were caused by alternative 3 instead of 1 or 2; and for $c_{f,MAX}$, the pattern between alternatives 1-5 is quite random.

Not all the changes are desirable, when the protection of the ruin fabric is in question. Mitigation of the studied extremes is favourable. Thus, for c_{pe}, lowering the maximum and upping the minimum values are preferable, and lowering the maximum values of c_f (minimum values cannot be lower than zero as we saw before). See Tab. 1 for the summary of the results in this light.

For the HM, the most positive results are yielded by the alternatives completely covering the surface; yet these alternatives are negative for the LW in $c_{pe,max}$ values. The second best are alternatives with a slight offset of the roof from the HM. They also lead in $c_{pe,min}$ for the WW and LW or $c_{f,max}$ of the WW; yet these are the absolute worst in cf,min values for the HM. For the WW (based on the small tangible results recorded by the methodology of this study), the most positive alternatives are the ones with a slight offset of the roof from the HM and the most negative are the alternatives that are small in size and far from the HM. For the LW, the alternative with a slight offset from the HM is thought to be positive (even more so in $c_{pe,max}$; yet too much of a distance may lead to a negative effect on the $c_{pe,min}$ or $c_{f,max}$ values).

Tab. 1 *Summary of the first and second most positive and negative results*

	HM				WW				LW			
	+		-		+		-		+		-	
	#1	#2	#1	#2	#1	#2	#1	#2	#1	#2	#1	#2
$c_{pe,min}$	D1-H1	H2	A4	A5	D2	H2	A4	A5	H2	D3	A5	H5
$c_{pe,max}$	D1-H1	H2	A3	A4	*	*	*	*	H3	H4	H1	A2
$c_{f,min}$	D1-H1	*	H2	H3	*	*	*	*	*	*	*	*
$c_{f,max}$	D1-H1	D2	A4	A5	H1	D2	A5	A1	H1	D1	H3	H5
	* near zero, or otherwise insignifact values *											

4 DISCUSSION

Tangible patterns of the development of the values of the mean changes in the values of the exterior pressure and surface friction coefficients were obtained where expected; i.e., $c_{pe,min,diff}$, $c_{f,min,diff}$ and $c_{f,MAX,diff}$ on the HM surfaces, where the wind flow generally causes negative pressure and where its stream may flow in a parallel direction to the surface; $c_{pe,MAX,diff}$ and $c_{f,MAX,diff}$ on WW surfaces, generally the faces are stressed by positive pressure and zones where the stream splits from the centre of the windward face outwards to the edges. On LW surfaces, which are generally stressed by negative pressure, readable values of the mean changes were unexpectedly obtained in $c_{pe,MAX,diff}$ and $c_{f,MAX,diff}$, although they are not as clean as the results on previous zones of interest. More detailed attention to LW surfaces, for example, in terms of splitting this zone into side and back walls may be useful, although this might only be effective for orthogonal geometries of the model and perpendicular directions of the wind flow.

The tangible results point to the benefit of the positions of a large covering roof directly on the ruin or close to it in terms of the external pressure (Figs. 5, 6). However, such alternatives caused the most negative results in terms of the surface friction (Fig. 7). As for the surface of the head of the masonry (HM), no optimal alternative of the roof was found by this study, except for the alternatives in absolute contact with the ruin and which completely cover this area (see also Tab. 1).

The large alternatives with total or near contact caused the most negative effect on the windward faces of the ruin in the terms of external pressure (although not too significant in their real value; see Fig. 10) and the most positive effect in terms of the surface friction (see Fig. 12). The alternatives also resulted in a positive effect on the surface friction of the leeward faces (Fig. 16), although further distance is needed for a more positive effect on the external pressure (Fig. 14) (see also Tab. 1).

The results of the study of the extremes point to some contradictions. The alternatives positively affecting the external pressure result in a negative effect on the surface friction. Further research is recommended. Furthermore, the alternatives that are positive for one zone of interest on the surface of the ruin are negative for the other zones. Henceforth, a general view of the entire surface of the model and on each face of the ruin is not recommended. Introducing new subsections of zones of interests, such as horizontal stripes for the vertical faces of the model is a possible way to achieve an appealing level of detail. In moving forward from the idealised general state of the model (see Fig. 2), some levels of detail may be reintroduced in the model in order to distinguish one face from the other.

5 CONCLUSION

The study analysed how changing the size and distance of a flat roof over a ruin affects its capability to protect the ruin from destructive wind-induced mechanisms. The minimum and maximum values of the external pressure and the skin friction coefficients were considered. By focusing on their changes on the zones of the ruin surface, the degree of protection of the ruin by various alternatives of the flat roof was estimated. The study failed to identify the optimal flat roof alternative to cover the ruin in question. However, two specific aspects of the flat roof became of interest, i.e., the first one being the total contact of the roof with the ruin with a large overhang and the second one being a slight offset of the roof from the ruin. Both alternatives are questionable, depending on the preference of the specifics of the protection of the ruin's fabric. The positive effect in one phenomenon studied yielded negative results in the other area. Further research and scaling of the method is recommended.

REFERENCES

ANTROP, Marc, 2006. *Sustainable landscapes: Contradiction, fiction or utopia? Landscape and Urban Planning. 2006.* Vol. 75, Nos. 3-4, pp. 187-197. DOI 10.1016/j.landurbplan.2005.02.014.

ASLAN, Zaki, COURT, Sarah, TEUTONICO, Jeanne Marie and THOMPSON, Jane (eds.), 2018. *Protective Shelters for Archaeological Sites: Proceedings of a symposium (Herculaneum, Italy, 23-27 Sept 2013).* GB: The British School at Rome, London. ISBN 978-0-904152-79-1.

BIELEK, Boris, FRANEK, Michal and BIELEK, Milan, 2020. *Aerodynamics and hydrodynamics of buildings: Physical problematics of effect of wind and wind-driven rain on buildings and structures.* SR: Slovak University of Technology in Bratislava. ISBN 978-80-227-5051-6.

BRÁNICKÝ, F. and GREGOROVÁ, J., 2022. *Searching for lost identity of Orava countryside.* In: PEŘINKOVÁ, M., JÜTTNEROVÁ, S. and VIDECKÁ, L., 14th Architecture in Perspective 2022. Ostrava, CZ: VŠB - Technical University of Ostrava. 2022. pp. 84-89.

CABELLO-BRIONES, Cristina, MAYORGA-PINILLA, Santiago and VÁZQUEZ-MOLINÍ, Daniel, 2020. *Particulate dry deposition on sheltered archaeological remains: Considerations based on Complutum, a Roman site in Spain.* Journal of Cultural Heritage. 2020. Vol. 46, pp. 218-225. DOI 10.1016/j.culher.2020.07.005.

D'ACCI, Luca, 2019. *A new type of cities for liveable futures. Isobenefit Urbanism morphogenesis.* Journal of Environmental Management. Online. 2019. Vol. 246, pp. 128-140. [Accessed 9 May 2023]. DOI 10.1016/j.jenvman.2019.05.129.

FORTUNATO, Giuseppe, FREGA, Ferdinando, LAURIA, Agostino and ZAPPANI, Antonio Agostino, 2024. *Documenting and analysing to preserve: An integrated approach between laser scanning and Computational Fluid Dynamics.* The case study of the column of the temple of Hera Lacinia near Crotone. Journal of Cultural Heritage. Online. 2024. Vol. 66, pp. 244-253. [Accessed 27 Sept 2024]. DOI 10.1016/j.culher.2023.11.020.

FOUAD, N. S., MAHMOUD, G. H. and NASR, N. E., 2018. *Comparative study of international codes wind loads and CFD results for low rise buildings.* Alexandria Engineering Journal. 2018. Vol. 57, no. 4, pp. 3623-3639. DOI 10.1016/j.aej.2017.11.023.

GREGOROVÁ, Jana and VOJTEKOVÁ, Eva, 2022. *Preparation of complex renovation of national cultural monument of the fortification of the town Trnava: Pilot project of the UNESCO chair for preservation of the architectural heritage at the Slovak university of technology in Bratislava (1st phase).* Archinfo. Online. 2022. [Accessed 5 March 2023]. Retrieved from: www.archinfo.sk/diskusia/blog/diela/priprava-komplexnej-obnovy-nkp-mestskeho-opevnenia-v-trnave-pilotny-projekt-katedry-unesco-pre-obnovu-architektonickeho-dedicstva-na-stu-v-bratislave-1-etapa.html

HOW, C., 2007. *Stability and survival.* In: ASHURST, John, Conservation of Ruins. UK: Butterworth-Heinermann. pp. 11-43. ISBN 978-0-75-066429-5.

HUSSEIN, A. S. and EL-SHISHINY, H., 2009. *Wind flow modeling and simulation over the Giza Plateau cultural heritage site in Egypt.* Journal on Computing and Cultural Heritage. 2009. Vol. 2, no. 2, pp. 1-22. DOI 10.1145/1613672.1613674.

KIM, YunSang, 2023. *Evaluating environmental factors using microclimate survey and computer fluid dynamics analysis of Korean traditional wooden architectural cultural heritage: focusing on the Kim Myeong-KwanGotaek.* Heritage Science. Online. 2023. Vol. 11, no. 1. [Accessed 27 Sept 2024]. DOI 10.1186/s40494-023-00951-2.

MAKÝŠ, Oto, 2018. *Technology of building renovation: Implementation of renovation of cultural monuments.* SK: Spektrum STU, Bratislava. ISBN 978-80-227-4880-3.

MOU, B., HE, B., ZHAO, D. and CHAU, K., 2017. N*umerical simulation of the effects of building dimensional variation on wind pressure distribution.* Engineering Applications of Computational Fluid Mechanics. 1 Jan 2017. Vol. 11, no. 1pp. 293-309. DOI 10.1080/19942060.2017.1281845.

PINEDA, PP. and IRANZO, A., 2017. *Analysis of sand-loaded air flow erosion in heritage sites by Computational Fluid Dynamics: Method and damage prediction.* Journal of Cultural Heritage. 2017. Vol. 25, pp. 75-86. DOI 10.1016/j.culher.2016.12.005.

POLIAK, Martin, 2022. *Geometry analysis of ruin-coverage contact.* In: Advances in Architectural, Civil and Environmental Engineering. Bratislava, SK: Spektrum STU. 2022. pp. 365-372. ISBN 97-80-227-5251-0.

POLIAK, Martin, FRANEK, Michal and GREGOROVÁ, Jana, 2023. *Evaluation of a Measurement Turbulence Model of the Wind Pressure on the Ruin of a Fortified Tower.* Slovak Journal of Civil Engineering. Online. 1 June 2023. Vol. 31, no. 2, pp. 25-36. [Accessed 19 June 2024]. DOI 10.2478/sjce-2023-0010.

POLIAK, Martin, GREGOROVÁ, Jana and (eds.), 2022. *The impact of roofing a ruin on the methodology of its presentation in relation to exposure.* In: PEŘINKOVÁ, Martina, JÜTTNEROVÁ, Sandra and VIDECKÁ, Lucie, 14th Architecture in Perspective. Ostrava: Technical University of Ostrava, Faculty of Civil Engineering, Department of Architecture. 2022. pp. 179-183. ISBN 978-80-248-4646-0.

RUHIGOVÁ, Ema, RUHIG, Roman and GREGOROVÁ, Jana, 2024. *Preservation of cultural diversity and current tools of monument care.* Muzeológia a kultúrne dedičstvo. Online. 2024. Vol. 12, no. 1, pp. 63-83. [Accessed 27 Sept 2024]. DOI 10.46284/mkd.2024.12.1.4.

SABBIONI, Cristina, BRIMBLECOMBE, Peter and CASSAR, Mark, 2010. *The atlas of climate change impact on European cultural heritage: Scientific Analysis and Management Strategies.* UK: Anthem Press. ISBN 978-92-79-09800-0.

SESANA, Elena, GAGNON, Alexandre S., CIANTELLI, Chiara, CASSAR, JoAnn and HUGHES, John J., 2021. *Climate change impacts on cultural heritage: A literature review.* WIREs Climate Change. Online. 2021. Vol. 12, no. 4 [Accessed 28 July 2021]. DOI 10.1002/wcc.710.

SHAO, Mingshen, LI, Li, WANG, Sijing, WANG, Enzhi and LI, Zuixiong, 2013. *Deterioration mechanisms of building materials of Jiaohe ruins in China.* Journal of Cultural Heritage. 2013. Vol. 14, no. 1, pp. 38-44. DOI 10.1016/j.culher.2012.03.006.

SINGH, J. and ROY, A. K., 2019. *Effects of Roof Slope and Wind Direction on Wind Pressure Distribution on the Roof of a Square Plan Pyramidal Low-Rise Building Using CFD Simulation.* International Journal of Advanced Structural Engineering. 2019. Vol. 11, no. 2, pp. 231-254. DOI 10.1007/s40091-019-0227-3.

Skin friction coefficient, CFD Online. Online. [Accessed 15 April 2023]. Retrieved from: www.cfd-online.com/Wiki/Skin_friction_coefficient

SORIA, Francisco J., GUERRERO, Luis F. and GARCÍA, Alma B., 2017. *Protective roof systems for archeological sites in Mexico.* In: WIT Transactions on the Built Environment. WITPress. pp. 225-236.

VECCO, M., 2020. *Genius loci as a meta-concept.* Journal of Cultural Heritage. 2020. Vol. 41, pp. 225-231. DOI 10.1016/j.culher.2019.07.001.

YAKA ÇETIN, Funda and IPEKOĜLU, Başak, 2013. *Impact of transparency in the design of protective structures for conservation of archaeological remains.* Journal of Cultural Heritage. 2013. Vol. 14, no. 3, pp. 21-24. DOI 10.1016/j.culher.2012.10.019.